ĐẠI HỌC QUỐC GIA HÀ NỘI
TRƯỜNG ĐẠI HỌC KHOA HỌC TỰ NHIÊN
**KHOA TOÁN CƠ TIN HỌC**

**Nguyễn Ngọc Hải**

# Mô hình toán học và cá thể hóa trong điều trị tiểu đường

Ngành Toán học
Chương trình Cử nhân Khoa học tài năng

**Hà Nội - 2023**

VIETNAM NATIONAL UNIVERSITY, HANOI
VNU UNIVERSITY OF SCIENCE
**FACULTY OF MATHEMATICS - MECHANICS - INFORMATICS**

**Nguyen Ngoc Hai**

# Mathematical Modeling to Analyze Diabetes and Optimize Personally Insulin Bolus Therapy

Submitted in partial fulfillment of the requirements for the degree of Bachelor of Science in Mathematics
(Talented Program)

**Hanoi - 2023**

VIETNAM NATIONAL UNIVERSITY, HANOI
VNU UNIVERSITY OF SCIENCE
**FACULTY OF MATHEMATICS - MECHANICS - INFORMATICS**

**Nguyen Ngoc Hai**

# Mathematical Modeling to Analyze Diabetes and Optimize Personally Insulin Bolus Therapy

Submitted in partial fulfillment of the requirements for the degree of Bachelor of Science in Mathematics
(Talented Program)

**Supervisor: Dr. Nguyen Trong Hieu**

**Hanoi - 2023**

# Acknowledgment

I would like to express my appreciation to my supervisor Dr. Trong Hieu Nguyen. He has provided valuable advice and insightful suggestions for me to accomplish my goal in the thesis. Dr Hieu has given me the opportunity to explore the world of Mathematics.

I also want to thank my family and friends who has always been encourage me to search for inspiration in Mathematics. Thank my academic advisor, Associate Professor Dr. Nhat Huy Vu, for his support throughout my 4 years of undergraduate study.

Due to the limited time and resources, the thesis can not be perfect. I truly hope to receive constructive comments and suggestions from anyone interested in my thesis.

Hanoi, May 2023

Ngoc Hai Nguyen

# Contents

# List of Figures

# Chapter 1

# Overview

## 1.1 Motivation

Diabetes, a chronic metabolic disorder, is one of the most widespread diseases of the 21st century, with a staggering 422 million individuals worldwide suffering from related conditions. In Vietnam, the number of individuals afflicted with diabetes is 5 million and continues to rise. It is estimated that over 422 million people globally are living with diabetes and that number is projected to continue to rise in the coming years. There are several risk factors associated with the development of diabetes, including family history, obesity, physical inactivity, and an unhealthy diet high in sugar and saturated fats. Traditional treatment and monitoring methods of diabetic patients using insulin pumps have encountered difficulties as the dosage is estimated based on external physical observations and does not reach optimal accuracy. In recent years, personalized medicine has gained considerable attention, and as a result, research and treatment of diabetes have been the focus of increased interest. Creating a mechanism simulation of diabetes, upon which numerous surveys and predictions can be conducted, is a logical

next step. While previous studies, such as those done by [1], [2], [3], [8], have been conducted on modeling diabetes, there is still considerable room for exploration. Therefore, in this thesis, based on previous research results and the author's own efforts, a new mathematical model is proposed to analyze the fundamental mechanism of diabetes, with a focus on the interaction between insulin and glucose. The ultimate objective of this model is to provide a method of controlling insulin delivery into the body to optimize treatment efficiency and improve patient outcomes.

This thesis is organized into several sections. Chapter 2 provides an overview of the basic knowledge about diabetes, including its underlying causes and contributing factors. Chapter 3 proposes a mathematical model that focuses on the relationship between insulin and glucose and compares it with existing models. Chapter 4 discusses the estimation of parameters, including specific methods and techniques used, followed by a presentation of simulation tests. The simulation results are shown in Chapter 5. Chapter 6 introduces an optimal insulin control method, detailing its effectiveness and comparing it with traditional treatment methods. Finally, Chapter 7 provides concluding remarks and further discussion on potential areas for future research and development. It is hoped that this study will contribute to the improvement of diabetes treatment and management, ultimately leading to better patient outcomes and quality of life.

## 1.2 Preliminaries

### 1.2.1 Biological Module of Diabetes

Diabetes mellitus is a chronic metabolic disorder characterized by persistently elevated levels of blood glucose. This condition arises due to either insufficient insulin production or the body's inability to effectively utilize insulin. Insulin, a hormone synthesized by the pancreas, plays a pivotal role in regulating blood glucose concentrations. Type 1 diabetes is marked by an absence of insulin production, whereas type 2 diabetes is characterized by insulin resistance.

To elucidate the vital roles of glucose and insulin in the human body, we first provide a brief overview of their functions. Figure 1.1 depicts a simplified block diagram illustrating the significance of glucose and insulin in human metabolism. Glucose, a carbohydrate found in various foods, serves as the primary energy source for the body's cells. Through glycolysis and other metabolic pathways, glucose is converted into adenosine triphosphate (ATP), the energy currency of the cell.

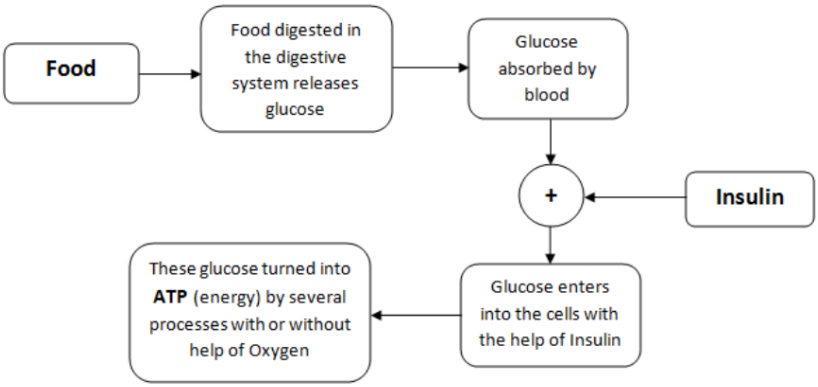


Figure 1.1: Insulin's mode of action

In certain cells, glucose is metabolized into energy in the presence of oxygen, while in others, it is converted to energy anaerobically. Insulin is crucial in this process, as it facilitates glucose entry into cells. If insulin levels are insufficient or if body cells exhibit insulin resistance, glucose cannot be efficiently utilized, leading to elevated blood glucose levels and subsequent complications. Figure 1.2 demonstrates how the body maintains blood glucose concentrations within a normal range.

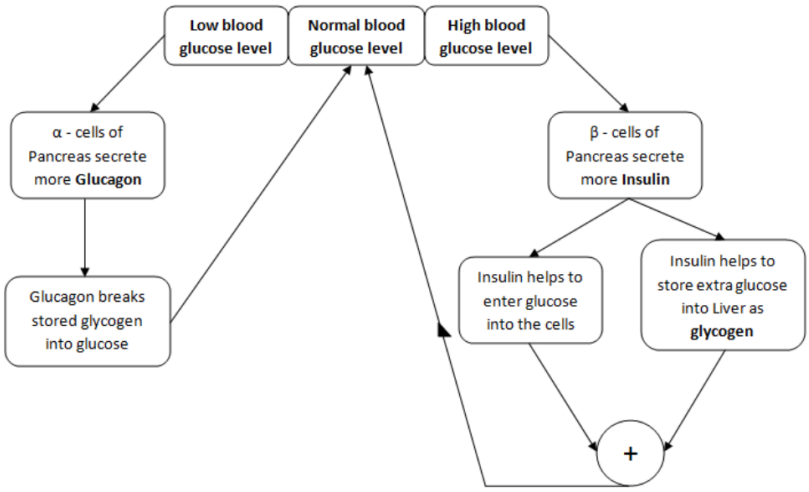


Figure 1.2: Blood glucose homeostasis

When blood glucose concentrations are high, the pancreas' $\beta$-cells produce more insulin, promoting glucose uptake by cells for energy production, as depicted in Figure 1.2. Additionally, insulin aids in the storage of excess glucose in the liver as glycogen. Conversely, when blood glucose levels are low, $\alpha$-cells in the pancreas secrete glucagon, which breaks down stored glycogen into glucose, thereby restoring normal glucose levels. This dynamic system represents the homeostatic mechanism in a healthy individual. However, in diabetic patients, this process becomes impaired, as illustrated in Figure 1.3.

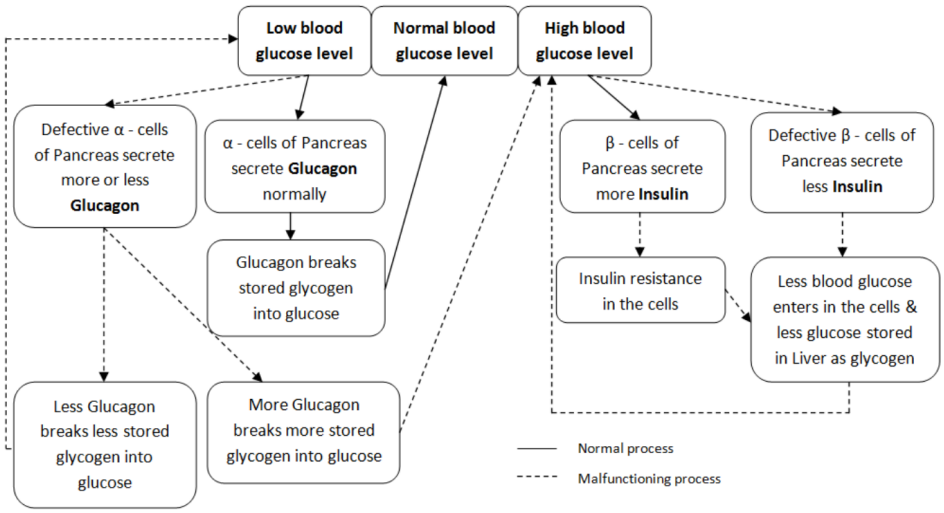


Figure 1.3: Dysregulated blood glucose homeostasis in diabetes

In summary, there are two primary instances in which the homeostatic system fails to function optimally. In type 1 diabetes, the individual's immune system, specifically T-cells, destroys the pancreas' $\beta$-cells, resulting in insufficient insulin production and consequently, persistently elevated blood glucose levels. In type 2 diabetes, cells in the body become resistant to insulin, leading to inadequate glucose uptake and reduced glycogen storage in the liver. The pancreas compensates by secreting excess insulin; if this surplus is sufficient to restore blood glucose levels to normal, the individual is considered pre-diabetic. If the elevated insulin secretion is inadequate, the person is diagnosed with type 2 diabetes. Additionally, dysfunctional $\alpha$-cells in the pancreas can contribute to elevated blood glucose levels by producing excessive glucagon.

In this thesis, we will develop a mathematical model based on the biological phenomena and events presented in Figures 1.1, 1.2, and 1.3

### 1.2.2 Diagnostic Test Methods

The Oral Glucose Tolerance Test (OGTT), meal tests, and Intravenous Glucose Tolerance Test (IVGTT) are diagnostic methods employed to assess an individual's glucose metabolism and insulin sensitivity. These tests provide valuable insights into how effectively the body processes glucose, helping to identify potential cases of diabetes, prediabetes, and other metabolic disorders.

- Oral Glucose Tolerance Test (OGTT): The OGTT is a widely used test to diagnose diabetes, prediabetes, and gestational diabetes. The test involves fasting for at least 8 hours, followed by the ingestion of a specific amount of glucose (typically 75 grams) dissolved in water. Blood samples are collected at multiple time points, including baseline (before glucose ingestion) and at intervals of 30 minutes, 1 hour, 2 hours, and sometimes 3 hours post-ingestion. The blood glucose levels at these time points are then analyzed to determine the body's ability to metabolize glucose. Elevated blood glucose levels at 2 hours suggest impaired glucose tolerance, which may indicate diabetes or prediabetes, depending on the degree of elevation.

- Meal Tests: Meal tests, also known as mixed meal tolerance tests (MMTT), assess glucose metabolism and insulin secretion in response to a mixed meal containing carbohydrates, proteins, and fats. This test provides a more physiologically relevant assessment of glucose homeostasis as it simulates real-life conditions. The individual consumes a standardized meal, and blood samples are collected at baseline and at

regular intervals (e.g., every 30 minutes) for several hours post-meal. Blood glucose and insulin levels are measured to evaluate the body's response to the meal, with particular attention to postprandial glucose excursions and insulin secretion patterns. Abnormal glucose or insulin responses may indicate impaired glucose metabolism or insulin dysfunction, potentially signaling diabetes or other metabolic disorders.

- Intravenous Glucose Tolerance Test (IVGTT): The IVGTT is a test that directly measures the body's response to a known amount of glucose administered intravenously. This test bypasses the gastrointestinal tract, allowing for a rapid and more controlled assessment of glucose metabolism and insulin sensitivity. After an overnight fast, a bolus of glucose is infused intravenously, and blood samples are collected at predetermined time points to measure glucose and insulin concentrations. The IVGTT can be a simple test, known as the Minimal Model IVGTT, or more complex, incorporating exogenous insulin administration as in the frequently sampled intravenous glucose tolerance test (FSIVGTT) or the hyperinsulinemic-euglycemic clamp. The results of the IVGTT help to quantify insulin sensitivity and glucose effectiveness, providing valuable information for diagnosing diabetes, insulin resistance, and other metabolic disorders.

In summary, the OGTT, meal tests, and IVGTT are critical diagnostic tools for evaluating glucose metabolism and insulin sensitivity in both clinical and research settings.

### 1.2.3 Related work

In [5], the research conducted by Bergman and colleagues provides a comprehensive understanding of the construction and evolution of kinetic mathematical models used in metabolism research related to diabetes.

Initially, the researchers focused on the fundamental aspects of glucose dynamics. In cases where the interplay between glucose and insulin is unknown, an insulin-independent approach is typically the most appropriate. The first simplistic approach involves assuming that glucose production remains constant, and that the rate of glucose utilization is a linear function of plasma glucose concentration. Denote $G(t)$ as glucose disturbance in the blood at time $t$ (mg/dl). This model can be expressed formally as

$$\frac{dG(t)}{dt} = p_1 G(t) + p_0 \tag{1.2.1}$$

which could be a little more medical specified by this version using Michaelis - Menten parameters. The Michaelis-Menten parameters are commonly used in enzymology to describe the behavior of enzymes that catalyze a reaction involving a substrate. The Michaelis-Menten equation relates the rate of enzyme-catalyzed reaction to the concentration of substrate. The Michaelis constant, $p_2$, is defined as the substrate concentration at which the reaction velocity is half of the maximum reaction velocity (i.e., when $[S] = p_2, v = \frac{V_{max}}{2}$). Thus, Michaelis-Menten parameter provides information about the efficiency of the enzyme-substrate interaction: a low value indicates a high affinity of the enzyme for its substrate, while a high value indicates a low affinity.

$$\frac{dG(t)}{dt} = \frac{p_1 G(t)}{p_2 + G(t)} + p_0 \tag{1.2.2}$$

A further think lead to the model capturing two compartment glucose distribution interact with each other. Here the second compartment represents the target cells and tissues where glucose is taken up and metabolized. Denote $X(t)$ as glucose disturbance in the second compartment at time $t$ (mg/dl), we have

$$\begin{aligned} \frac{dG(t)}{dt} &= p_1 G(t) + p_2 X(t) + p_3 \\ \frac{dX(t)}{dt} &= G(t) + p_4 X(t) \end{aligned} \tag{1.2.3}$$

A breakthrough exist when considering a model explaining the dependence of glucose's change on the existence of insulin. It could have the variants

- Glucose disappearance in this model is linearly dependent on both the plasma glucose and insulin concentrations. Glucose distributes in a single compartment, and the production is assumed constant

$$\frac{dG(t)}{dt} = p_1 G(t) + p_2 I(t) + p_0 \tag{1.2.4}$$

- Another model assumes that glucose uptake is directly depend on concentration of insulin, not in plasma, but in a second compartment of insulin distribution remote from plasma.

$$\begin{aligned} \frac{dG}{dt} &= p_1 G(t) + p_2 X(t) + p_3 \\ \frac{dX}{dt} &= p_4 X(t) + I(t) \end{aligned} \tag{1.2.5}$$

- It is also important to note that, in the model, alterations could be made to the interaction between two compartments that contain glucose

$$\begin{aligned} \frac{dG}{dt} &= (p_1 - X(t))\, G(t) + p_4 \\ \frac{dX}{dt} &= p_2 X(t) + p_3 I(t) \end{aligned} \tag{1.2.6}$$

Ultimately, Bergman and Cobelli arrived at a final model, known as the minimal model, which can be expressed as

$$\frac{dG(t)}{dt} = -\left[p_1 + X(t)\right] G(t) + p_1 G_b, G(0) = p_0 \tag{1.2.7}$$

$$\frac{dX(t)}{dt} = -p_2 X(t) + p_3 \left(I(t) - I_b\right), X(0) = 0 \tag{1.2.8}$$

$$\frac{dI(t)}{dt} = p_4 \left(G(t) - p_5\right)^+ t - p_6 \left(I(t) - I_b\right), I(0) = p_7 + I_b \tag{1.2.9}$$

where, $(G(t) - p_5)^+ = G(t) - p_5$ if $G(t) > p_5$ and 0 otherwise. $I(t)$ represents the effective insulin level at time $t$ ($\mu$U/ ml). In the context of modeling glucose uptake activity in insulin-excitable tissue, the function $X(t)$ serves as an auxiliary tool. The subject's baseline glycaemia and insulinemia are denoted as $G_b$ and $I_b$, respectively, while $p_1$ through $p_7$ represent various parameters. Notably, the equations 1.2.7 through 1.2.8 were originally developed for the purpose of characterizing FSIGT data, but they are composed of two distinct parts. The first part utilizes equations 1.2.7 and 1.2.8, while the second part relies solely on equation 1.2.9. While many studies have utilized modified versions of the glucose minimal model (equations 1.2.7 and 1.2.8) to analyze OGTT and meal tests, insulin minimal models derived from equation 1.2.9 have only been applied to IVGTT. It is important to emphasize that the glucose minimal model has been especially useful for estimating insulin sensitivity ($S_I = \frac{p_3}{p_2}$) without requiring glucose clamps.

Variant versions based on the minimal model were considered by different authors. An example of this category was proposed by Derouich and Boutayeb in [6] who used a modified version of the minimal model to introduce param-

eters related to physical exercise

$$\begin{aligned} \frac{dG(t)}{dt} &= -\left(1+q_2\right)X(t)G(t) + \left(p_1+q_1\right)\left(G_b - G(t)\right) \\ \frac{dX(t)}{dt} &= -p_2X(t) + \left(p_3+q_3\right)\left(I(t) - I_b\right), \end{aligned} \tag{1.2.10}$$

where, $q_1$ is the effect of physical exercise in accelerating the utilization of glucose by muscles and the liver insulin, $q_2$ is the effect of physical exercise in increasing the muscular and liver sensibility to the action of insulin, $q_3$ is the effect of physical exercise in increasing the utilization of insulin. In other words, $q_3$ increases insulin effectiveness in enhancing glucose disposal and consequently improving insulin sensitivity to become: $S_I = \frac{(p_3+q_3)(1+p_2)}{p_2}$. Overall, the glucose minimal model and its associated equations have proven to be valuable tools for understanding glucose uptake activity and insulin sensitivity, with potential applications in various testing scenarios. Despite its limitations, this model represents an important contribution to the field of glucose metabolism research.

# Chapter 2

# Mathematical Modelling

## 2.1 Criteria for Modelling

Balancing the need for a well-captured model with its complexity is a trade-off in mathematical modeling. A simpler model may not capture all aspects of the system, while a more complex model may be more accurate but difficult to interpret or computationally expensive. Based on our understanding, the biggest model consists of six equations, as mentioned in [15]. Finding the right balance depends on the specific application and available resources. Our goal is to build a model which is simple but captures well the phenomenon. Building upon Figures 1.1, 1.2, and 1.3, we establish a set of criteria to ensure that our mathematical model accurately captures the fundamental aspects of glucose-insulin metabolism. These criteria, which serve as a foundation for a "well-represented" model, can be outlined as follows:

(a) The quantities of glucose and insulin present in each compartment should be positive and finite at all times, reflecting the physiological constraints of the human body.

(b) Given sufficient time and in the absence of any external inputs, such

as glucose or insulin disturbances, the concentrations of glucose and insulin in each compartment should approach zero. This property ensures that the model exhibits a stable equilibrium state under normal conditions.

(c) The model should account for a time delay representing the period between food consumption and its subsequent conversion within the digestive system into glucose in the blood compartment. This delay reflects the inherent physiological processes involved in digestion and absorption.

(d) Blood glucose concentrations should primarily be regulated by the hormone insulin. However, the model should also consider the influence of insulin-independent factors that contribute to glucose clearance even in the absence of metabolism.

(e) Insulin can be divided into two components: basal insulin and rapid-acting insulin. Rapid-acting insulin is released only when blood glucose concentrations exceed a certain threshold, reflecting the body's response to elevated glucose levels.

(f) Over time, the amount of rapid-acting insulin should naturally decrease, representing the body's gradual return to a baseline state after the clearance of excess glucose.

By incorporating these criteria into the development of a mathematical model, we can ensure a more accurate representation of the underlying glucose-insulin dynamics within the human body. Such a model can serve as a

valuable tool for understanding and predicting the behavior of glucose and insulin in various scenarios, including those related to diabetes management and treatment.

## 2.2 Proposed Model

We summarize the information presented in the figures above and create a conceptual framework that captures the underlying models.

Let us denote the three main factors in our model as follows:

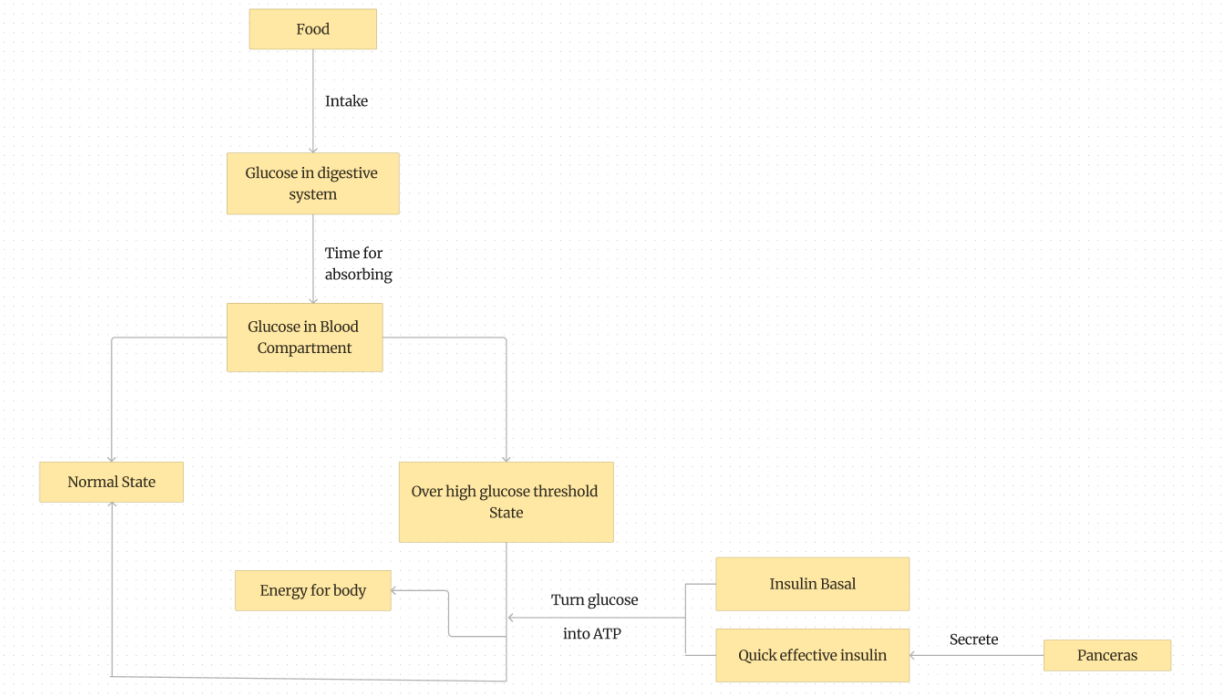


Figure 2.1: Knowledge of the model

- $G_1(t)$: Glucose disturbance of the digestive system at time $t$ (mg/dl)
- $G_2(t)$: Glucose disturbance in the blood at time $t$ (mg/dl)
- $I(t)$: The effective insulin level at time $t$ ($\mu$U/ ml)

Here, we decompose $I(t)$ into two components: basal insulin $I_b$ and rapid-acting insulin $\bar{I}(t)$. That is, $I(t) = I_b + \bar{I}(t)$. We propose a new dynamical system formulation as follows:

$$\begin{aligned}
\frac{dG_1(t)}{dt} &= -\alpha G_1(t) \\
\frac{dG_2(t)}{dt} &= \alpha G_1(t) - \left(\beta_1 + \beta_2 \left(\bar{I}(t) + I_b\right)\right) G_2(t) \\
\frac{d\bar{I}(t)}{dt} &= \gamma \ln\left(\exp\left(G_2(t) - T_{upper}\right) + 1\right) - \delta \bar{I}(t)
\end{aligned} \tag{2.2.1}$$

where

- $\alpha$ is the rate constant of decreasing glucose level in the digestive system (mg/dl/h)
- $\beta_1$ is the rate constant of the hormone-independent decrease of glucose level in the blood (mg/dl/h)
- $\beta_2$ is the rate constant of the hormone-dependent decrease of glucose level in the blood (mg/dl/h)
- $\gamma$ is the rate constant of release of the hormone due to blood glucose disturbance ($\mu$U/ml/h)
- $\delta$ is the rate constant for the removal of the hormone due to disturbance of the blood hormone level ($\mu$U/ml/h)
- $I_b$ is insulin basal level ($\mu$U/ml)
- $T_{upper}$ is the threshold for high blood glucose concentration (mg/dl)

We introduce an equation for the dynamics in the digestive system that represents the time delay between food in the stomach and glucose in the

blood, which corresponds to condition (c). The second and third equations in our model capture the phenomena described in conditions (d), (e), and (f).

To represent the appearance of insulin in condition (e), the ideal function would be $ReLU(G_2(t) - T_{upper})$. However, the ReLU function is not differentiable at point 0, which could pose challenges in future research development. Instead, we employ the softplus function $\ln(e^x + 1)$, which has a similar shape to the ReLU function but is smooth. This choice of function allows us to model the insulin release dynamics more accurately and with better mathematical properties.

We prove that, in a mathematical way, this system is valid. i.e, it has the solution that satisfies the condition (b). For the shake of simplicity in proof, we shorten write the equation as

$$\frac{dX(t)}{dt} = f(t, X) \tag{2.2.2}$$

with

$$X(t) = \left(G_1(t), G_2(t), \bar{I}(t)\right)$$

and

$$f(t, X) = \begin{pmatrix} -\alpha G_1(t) \\ \alpha G_1(t) - (\beta_1 + \beta_2 I(t))\, G_2(t) \\ \gamma \ln\left(\exp\left(G_2(t) - T_{upper}\right) + 1\right) - \delta \bar{I}(t) \end{pmatrix}$$

To begin with, we establish the unique existence of the solution $\bar{X}(t)$. This can be achieved by employing a well-known theorem.

**Theorem 2.2.1** (Picard's Existence Theorem)**.** *Consider the Initial Value Problem (IVP)*

$$x' = f(t, x), \quad x\left(t_0\right) = x_0$$

*Suppose* $f(t,x)$ *and* $\frac{\partial f}{\partial x}(t,x)$ *are continuous functions in some open rectangle* $\mathbb{R} \in \mathbb{R} \times \Omega$ *that contains the point* $(t_0, x_0)$. *Then the IVP has a unique solution in some closed interval* $I = [t_0 - h, t_0 + h]$, *where* $h > 0$. *Moreover, the Picard iteration defined by*

$$x_{n+1}(t) = x_0 + \int_{t_0}^{t} f\left(s, x_n(s)\right) ds$$

*produces a sequence of functions* $\{x_n(t)\}$ *that converges to this solution uniformly on* $I$.

Applying Picard's Theorem, we observe that all the component functions of $f(t, X)$ in equation 2.2.2 are smooth on their respective domains. Therefore, our model has solution. Moreover, it is unique due to Uniqueness Theorem

**Theorem 2.2.2** (Uniqueness)**.** *Suppose for some* $\alpha > 0$ *and some* $r > 0, f(t,x)$ *is Lipschitz continuous on* $I_\alpha \times \overline{B_r\left(x_0\right)}$, *and suppose* $x(t)$ *and* $y(t)$ *both are* $C^1$ *solutions of (IVP) on* $I_\alpha$, *where* $I_\alpha = [t_0, t_0 + \alpha]$. *Then* $x(t) = y(t)$ *for* $t \in I_\alpha$.

In order to analyze the constraints of variables and fixed points, the Comparison Theorem is required.

**Theorem 2.2.3** (Comparison Theorem)**.** *Let* $(t,x) \in \mathbb{R} \times \mathbb{R}$. *Suppose* $f(t,x)$ *is continuous in* $t$ *and* $x$ *and Lipschitz continuous in* $x$. *Suppose* $x(t), y(t)$ *are* $C^1$ *for* $t \geq t_0$ *(or some interval* $[t_0, b)$ *or* $[t_0, b]$ *) and satisfy*

$$x'(t) \leq f(t, x(t)), \quad y'(t) = f(t, y(t))$$

*and* $x(t_0) \leq y(t_0)$. *Then* $x(t) \leq y(t)$ *for* $t \geq t_0$.

Upon solving the first equation of 2.2.1, we obtain

$$G_1(t) = G_{10}e^{-\alpha t},$$

which implies that $G_1(t) \geq 0$. Moreover, while solving the equation

$$\frac{d\bar{I}}{dt} = -\delta I, I(0) = I_0,$$

we get the solution

$$\hat{I}(t) = I_0 e^{-\delta t}.$$

By the Comparison Theorem, we have

$$I(t) \geqslant \widehat{I}(t) > 0.$$

Similarly, we have

$$\frac{dG_2}{dt} \geqslant -\left(\beta_1 + \beta_2 \bar{I}\right) G_2,$$

which implies

$$G_2(t) \geqslant \widehat{G}_2(t) = G_{20}e^{-(\beta_1+\beta_2 I)t} > 0$$

with $\widehat{G}_2(t)$ being the solution of

$$\frac{d\hat{G}_2}{dt} = -\left(\beta_1 + \beta_2 I\right) G_2, G_2(0) = G_{20}.$$

To determine fixed points we can write,

$$\frac{dG_1(t)}{dt} = \frac{dG_2(t)}{dt} = \frac{d\bar{I}(t)}{dt} = 0$$

which turns into

$$\begin{cases} -\alpha G_1 = 0 \\ \alpha G_1 - \left(\beta_1 + \beta_2 \bar{I}\right) G_2 = 0 \\ \gamma \ln\left(\exp\left(G_2(t) - T_{upper}\right) + 1\right) - \delta \bar{I}(t) = 0 \end{cases}$$

From the first equation, we have

$$G_1 = 0$$

Putting into second equation

$$\left(\beta_1 + \beta_2 \bar{I}\right) G_2 = 0$$

Due to the positivity of $\beta_1 + \beta_2 \bar{I}$ we have

$$G_2 = 0$$

Finally, the third equation implies

$$\bar{I} = \frac{\gamma}{\delta} \ln(e^{-T_{upper}} + 1)$$

which is near to 0 due to the value of $T_{upper}$ usually being chosen around 100-120.

In conclusion, the proposed model, given by 2.2.1, fulfills all necessary criteria for an accurate and comprehensive representation. Its simplicity, relying on only three equations, offers a more streamlined approach compared to existing state-of-the-art models. Furthermore, to the best of our knowledge, this is the first model capable of optimizing the specific trade-off under discussion.

# Chapter 3

# Parameter Estimation

The proposed model requires the estimation of its parameters, which are currently unknown. The parameter estimation process is customized for each patient based on their personal data, including glucose levels in the digestive tract, blood, and insulin levels. This approach is known as personalization therapy in medical context. The error can be determined by comparing the actual observed data with the point-in-time solutions of the differential equation system, obtained using a specific set of parameters. However, exact solutions of many ODEs are difficult to obtain, and numerical techniques are often used to solve such ordinary differential equations.

## 3.1 Numerical Solving Ordinary differential equations

We utilize the Runge-Kutta method for our approach. Runge-Kutta method is a numerical method used to solve ordinary differential equations (ODEs) numerically [10]. It is based on the idea of approximating the solution at discrete points in time, and then using these approximations to find the solution at the next point in time. The main advantage of Runge-Kutta

method is that it is very accurate, and can be used to solve ODEs that do not have a closed-form solution.

The technique behind the Runge-Kutta method involves breaking up the interval of interest into smaller subintervals, and approximating the solution at each subinterval using a weighted average of function evaluations at various points within the subinterval. The weights are chosen in such a way as to minimize the error in the approximation.

The most commonly used Runge-Kutta method is the fourth-order method, which is also known as RK4. This method involves evaluating the function at four different points within the subinterval, and then taking a weighted average of these evaluations to obtain the approximation. The RK4 method is very accurate and is widely used in many fields, including engineering, physics, and mathematics.

Formally, consider initial value problem

$$\frac{du(t)}{dt} = f(t, u)$$

with $t$ from $t_0$ to $T$, $u(t_0) = u_0$, we have Runge-Kutta method of order 4 to solve this problem

**Algorithm 1** Runge-Kutta method of order 4

$t_n \leftarrow t_0$
$u_n \leftarrow u_0$
**while** $t_n < T$ **do**
    $h \leftarrow \min(h_{\max}, T - t_n)$
    $k_1 \leftarrow hf(t_n, u_n)$
    $k_2 \leftarrow hf(t_n + \frac{h}{2}, u_n + \frac{k_1}{2})$
    $k_3 \leftarrow hf(t_n + \frac{h}{2}, u_n + \frac{k_2}{2})$
    $k_4 \leftarrow hf(t_n + h, u_n + k_3)$
    $u_{n+1} \leftarrow u_n + \frac{1}{6}(k_1 + 2k_2 + 2k_3 + k_4)$
    $t_{n+1} \leftarrow t_n + h$
    $n \leftarrow n + 1$
**end while**
**return** $u(T)$

The main computational effort in applying the Runge-Kutta methods is the evaluation of $f$.The Runge-Kutta method of order four requires 4 evaluations per step, and the local truncation error is $O(h^4)$. For the higher order of Runge-Kutta method, e.g fifth-order Runge-Kutta; the main difference between the Runge-Kutta 4th order (RK4) and 5th order (RK5) methods lies in the number of evaluations of the function required for each step. RK4 requires 4 evaluations, while RK5 requires 6 evaluations. This means that RK5 is more accurate, but also more computationally expensive than RK4. Additionally, RK5 has a higher order error term, which means that it can maintain its accuracy over larger step sizes than RK4. However, RK4 is often still used due to its simplicity and efficiency.

**Algorithm 2** Runge-Kutta method of order 5

$t_n \leftarrow t_0$
$u_n \leftarrow u_0$
**while** $t_n < T$ **do**
    $h \leftarrow \min(h_{\max}, T - t_n)$
    $k_1 \leftarrow hf(t_n, u_n)$
    $k_2 \leftarrow hf(t_n + \frac{h}{5}, u_n + \frac{1}{5}k_1)$
    $k_3 \leftarrow hf(t_n + \frac{3h}{10}, u_n + \frac{3}{40}k_1 + \frac{9}{40}k_2)$
    $k_4 \leftarrow hf(t_n + \frac{4h}{5}, u_n + \frac{44}{45}k_1 - \frac{56}{15}k_2 + \frac{32}{9}k_3)$
    $k_5 \leftarrow hf\left(t_n + \frac{8}{9}h, u_n + \frac{19372}{6561}k_1 - \frac{25360}{2187}k_2 + \frac{64448}{6561}k_3 - \frac{212}{729}k_4\right)$
    $k_6 \leftarrow hf\left(t_n + h, y_n + \frac{9017}{3168}k_1 - \frac{355}{33}k_2 + \frac{46732}{5247}k_3 + \frac{49}{176}k_4 - \frac{5103}{18656}k_5\right)$
    $u_{n+1} \leftarrow u_n + \frac{35}{384}k_1 + \frac{500}{1113}k_3 + \frac{125}{192}k_4 - \frac{2187}{6784}k_5 + \frac{11}{84}k_6$
    $t_{n+1} \leftarrow t_n + h$
    $n \leftarrow n + 1$
**end while**
**return** $u(T)$

We need to modify a little for adaptation (Dorman Prince method). The Dorman Prince method has an embedded fifth-order method that can be used to estimate the error of the fourth-order method. This allows the step size to be adjusted automatically to maintain a desired level of accuracy. The method is also designed to be stable and robust, and it can handle stiff ODEs that are difficult to solve with other methods.

**Algorithm 3** Dorman-Prince method

$t_n \leftarrow t_0$
$u_n \leftarrow u_0$
**while** $t_n < T$ **do**
    $h \leftarrow \min(h_{\max}, T - t_n)$
    $k_1, k_2, k_3, k_4, k_5, k_6 \leftarrow$ **Fifth-order Runge-Kutta update**
    $u_{n+1} \leftarrow$ **Fifth-order Runge-Kutta update**
    $u_{\text{hat}} \leftarrow$ **Fourth-order Runge-Kutta update**
    $t_{n+1} \leftarrow t_n + h$
    $n \leftarrow n + 1$
    $e_n \leftarrow u_{\text{hat}} - u_{n+1}$
    **if** $|e_n| > \text{TOL}$ **then**
        $h \leftarrow \frac{h}{2}$
        **continue** ▷ Retry with a smaller step size
    **end if**
    $\text{TOL} \leftarrow 0.84 \left(\frac{\text{TOL} \cdot h}{|e_n|}\right)^{0.25}$ ▷ Adapt the tolerance
    $u_n \leftarrow u_{n+1}$
**end while**
**return** $u(T)$

## 3.2 Parameter Estimation for Ordinary Differential Equation

Using the Runge-Kutta methodology, we can generate a graph of $X(t)$ over time from 2.2.2 for a given parameter $\boldsymbol{p}$ and initial value $X(0) = X_0$. We meet a challenge that observations are only available for a subset of the components of $X(t)$ (i.e. $G_2(t)$ in this case. Continuous measurement of insulin over time is costly). Our objective is to determine an appropriate value for $\theta$ that produces a simulation of $G_2(t)$ that best fits the observed data $\left(G_2^{\text{obs}}(t_i), i = 1, \ldots, n_0\right)$.

Given such data, parameter estimation for ODEs is traditionally done using maximum likelihood estimation (MLE) .i.e solving nonlinear least square

problem

$$\min_{p} \sum_{i=1}^{n} q_G \frac{||G_2(t_i, p) - G_2^{\text{obs}}(t_i)||^2}{2} = \min_{p} \mathcal{L}(p)$$

However, non-linear least squares problems may be challenging because:

- The system needs to be approximated by using a numerical method.
- A good initial guess for $\hat{\boldsymbol{p}}$ is unavailable (only know broad ranges that parameters can take)

We evade these problems by a procedure including two stage like in [4]; in there first stage find a suitable initial guess $\boldsymbol{p_0}$ while the second stage apply a local, fast converging optimization to obtain $\hat{\boldsymbol{p}}$. This first stage is similar to the ideas of proposal generation in computer vision or a warm start when training neural networks, which can use a heuristic global search to solve an alternative optimization problem. The local optimizer is used in the second stage, since this is a Non-Linear Square problem, one might use a Gauss-Newton algorithm.

### 3.2.1 First stage - Finding an initial guess

Global optimization algorithms aim to find the global optimum solution, which is the best possible result within the feasible solution space. The process of finding this solution involves iteratively improving an initial point until the optimal solution is reached. The initial point serves as the starting point for the optimization process and has a significant impact on the success of the algorithm. A well-chosen initial point can lead to faster convergence to the global optimum solution, improving the accuracy and efficiency of the optimization process. On the other hand, a poorly chosen initial point can

result in convergence to a sub-optimal solution, reducing the effectiveness of the optimization algorithm. For example, an initial point that is too far from the global optimum solution may require a large number of iterations to reach the optimal solution, or may not converge at all.

Therefore, it is important to carefully choose an appropriate initial point in global optimization algorithms. This can be done by using prior knowledge about the problem, such as the location of local optima and the shape of the solution space. It can also be done by using various techniques such as random sampling, heuristics, or sophisticated methods such as genetic algorithms or simulated annealing. [9] proposed an approach called Smooth and Match Estimator (SME) to find an appropriate starting point $\boldsymbol{p}_{\text{sme}}$ through an optimization problem

$$\boldsymbol{p}_{\text{sme}} = \arg\min_{\boldsymbol{p}} \int_0^T \left\| \left( \tilde{\boldsymbol{G}_{\boldsymbol{2}}}'(t) - \boldsymbol{G}_2(t, \boldsymbol{p}) \right) \right\|^2 dt \tag{3.2.1}$$

where $\tilde{\boldsymbol{G}_{\boldsymbol{2}}}'(t)$ is obtained by smoothing the observations by spline or kernel regression. The mathematical technique behind the Smooth and Match Estimator (SME) involves a two-step process: smoothing the data and then estimating the parameters of the model. In the first step, the data is smoothed using a smoothing algorithm such as a spline regression. The purpose of this step is to reduce the impact of measurement error on the estimation process and improve the accuracy of the estimates. The smoothing algorithm involves fitting a smooth curve to the data, which can be used to represent the underlying relationships between the variables in the model.

We know that polynomial regression can produce smooth curves, but it is trained globally, which may not always be desirable. On the other hand,

step functions are trained locally but the resulting fits can be "bumpy," making them less useful in certain applications. To address these limitations, regression splines provide a solution by offering adaptive local smoothness. For overview of spline regression, its basis is piecewise polynomial regression. Piecewise polynomials are not fitted over the entire range but over different regions of data. Formally, we know the piecewise polynomial regression

$$y_i = \begin{cases} \beta_{01} + \beta_{11}x_i + \beta_{21}x_i^2 + \beta_{31}x_i^3 + \ldots + \beta_{d1}x_i^d + \epsilon_i, \text{ if } x_i < c \\ \beta_{02} + \beta_{12}x_i + \beta_{22}x_i^2 + \beta_{32}x_i^3 + \ldots + \beta_{d2}x_i^d + \epsilon_i, \text{ if } x_i \geq c, \end{cases}$$

where $i = 1, \ldots, n$ in both cases. A knot represents the cutpoint where two different LS fits are required: one for the samples where $x < c$ and one for the samples where $x \geq c$. Therefore, the knot determines the breakpoints of the piecewise polynomial. If there is no knot, then the regression is equivalent to standard polynomial regression. In general, if we have $K$ knots we are fitting $K + 1$ polynomial models. Using more knots leads to more flexible polynomial. This increases the flexibility of the model, but of course, too many knots can lead to overfitting. For the choice of degree of polynomials, we often consider

- Linear piecewise:

$$y = \begin{cases} \beta_{01} + \beta_{11}x, \text{if} x_i < c, \\ \beta_{02} + \beta_{12}x, \text{if} x_i \geq c. \end{cases}$$

- Cubic piecewise:

$$y = \begin{cases} \beta_{01} + \beta_{11}x + \beta_{21}x^2 + \beta_{31}x^3, \text{ if } x_i < c, \\ \beta_{02} + \beta_{12}x + \beta_{22}x^2 + \beta_{32}x^3, \text{ if } x_i \geq c \end{cases}$$

Here, for simplicity we consider the case there is only one knot. The quadratic case is generally not taken into account since it is typically outperformed by

the cubic case for complex data structures, and it does not show a significant improvement compared to the linear case for simpler data structures. In general, the cubic piecewise function is commonly preferred.

In conclusion, the SME method requires the specification of the smoothing algorithm and the estimation method, and the choice of these methods can have a significant impact on the performance of the SME. The SME method has been shown to be particularly useful in situations where the data is noisy or there is a large amount of measurement error, and has been applied in various fields including econometrics, engineering, and biology.

### 3.2.2 Second Stage

In the second stage, we use the notation

$$J_i(p) = G_2^{\text{obs}}(t_i) - G_2(t_i, \boldsymbol{p})$$
$$J(p) = (J_1, J_2, ..., J_n)^T,$$

so the loss function can be written as

$$\mathcal{L}(p) = \frac{1}{2}\sum_{i=1}^{n} J_i^2 = \frac{1}{2}||J||_2^2$$

The Gauss-Newton method is a simplification or approximation of the Newton method that applies to functions $\mathcal{L}$. Recall that Newton method reads the update at iteration $k+1$ as

$$\mathbf{p}^{(k+1)} = \mathbf{p}^{(k)} - \left(\nabla^2 \mathcal{L}\left(\mathbf{p}^{(k)}\right)\right)^{-1} \nabla \mathcal{L}\left(\mathbf{p}^{(k)}\right) \tag{3.2.2}$$

The drawback of Newton algorithm is the lack of the robustness, due to its update direction $d^{(k)} = -\nabla^2 \mathcal{L}\left(\mathbf{p}^{(k)}\right)^{-1} \nabla \mathcal{L}\left(\mathbf{p}^{(k)}\right)$ can not guarantee a descent direction. Gauss-Newton method is a upgrade version which can deal with

this problem. For specific, from initial point $p_0$, at step $k$, Gauss-Newton reads the update:

$$p^{(k+1)} = p^{(k)} - \alpha^{(k)} \cdot d^{(k)} \tag{3.2.3}$$

where

$$\mathbf{d}^{(k)} = - \left( \nabla J^T(p^{(k)}) \cdot \nabla J(p^{(k)}) \right)^{-1} \nabla \mathcal{L} \left( \mathbf{x}^{(k)} \right),$$

and $\alpha^{(k)}$ is the learning rate. We could show that this choice of update is reasonable. For all $k$, differtiating with respect to $p_k$ gives

$$\frac{\partial \mathcal{L}}{\partial p_k} = \sum_{i=1}^{n} \frac{\partial J_i}{\partial p_k} J_i,$$

which leads to the gradient of $\mathcal{L}$

$$\nabla \mathcal{L} = \nabla J^T(p) \cdot J(p).$$

Differentiating again with respect to $p_l$, we have $\forall k, l$

$$\frac{\partial^2 \mathcal{L}}{\partial p_k \partial p_l} = \sum_{i=1}^{n} \left( \frac{\partial J_i}{\partial p_k} \frac{\partial J_i}{\partial p_l} + J_i \frac{\partial^2 J_i}{\partial p_k \partial p_l} \right),$$

which yield the Hessian of $\mathcal{L}$

$$\nabla^2 \mathcal{L}(p) = \nabla J^T(p) \cdot \nabla J(p) + Q$$

where

$$Q = \sum_{i=1}^{n} J_i \nabla^2 J_i$$

The Gauss-Newton method is the result of neglecting the term $Q$, i.e., making the approximation $\nabla^2 \mathcal{L}(p) \approx \nabla J^T(p) \cdot \nabla J(p)$. Now we have the new search direction at iteration $k$

$$\mathbf{d}^{(k)} = - \left( \nabla J^T(p^{(k)}) \cdot \nabla J(p^{(k)}) \right)^{-1} \nabla \mathcal{L} \left( \mathbf{x}^{(k)} \right),$$

which implies a true descent direction. Note that $\nabla J^T(p^{(k)}) \cdot \nabla J(p^{(k)})$ has full rank so its transverse matrix exists. Indeed, we have

$$\nabla \mathcal{L}\left(\mathbf{p}^{(k)}\right)^T \mathbf{d}^{(k)} = -\nabla \mathcal{L}\left(\mathbf{p}^{(k)}\right)^T \left(\nabla J^T(p^{(k)}) \cdot \nabla J(p^{(k)})\right)^{-1} \nabla \mathcal{L}\left(\mathbf{x}^{(k)}\right) \leq 0.$$

This is because $\nabla J^T(p^{(k)}) \cdot \nabla J(p^{(k)})$ is positive semi-definite, which implies that $\left(\nabla J^T(p^{(k)}) \cdot \nabla J(p^{(k)})\right)^{-1}$ is also semi-define. Moreover, if the elements of $Q$ are small as we approach a minimum, we can expect fast convergence like Newton method 3.2.2. So the update formula 3.2.3 is valid.

The Gauss-Newton algorithm has several advantages, including its fast convergence rate, its ability to handle large data sets, and its ability to handle non-linear functions with high accuracy. However, it has some limitations, including its sensitivity to the choice of initial guess (which is solved by the first stage procedure) and its requirement for the Jacobian matrix to be positive definite.

## 3.3 Simulation

### 3.3.1 Data

The data used in this study were sourced from the Awesome-CGM repository [13], which provides links to publicly available continuous glucose monitoring (CGM) data by Mary Martin et.al. CGMs are wearable devices that allow for the continuous measurement of glucose levels throughout the day, with some devices taking measurements as often as every 15 minutes. The dataset chosen for analysis is the Appelo (2017) dataset, which includes 225 participants with type I diabetes aged between 25-40 over a period of 6 months, with visits every 3 weeks. The Dexcom G4 CGM device was used to collect glucose level data in this study. The Dexcom G4 is a small, wearable device that measures glucose levels in the interstitial fluid and transmits the readings wirelessly to a receiver, which displays the glucose levels in real-time and provides alerts for high or low glucose levels. The Dexcom G4 is designed to assist individuals with diabetes in managing their blood sugar levels more effectively and avoiding hypoglycemia and hyperglycemia. The dataset format is a txt file which is illustrated in Figure 3.1. In column 5th, there is a record of the time required for the CGM test, while in column 6th, the blood glucose level result is a crucial factor.

```
RecID|PtID|ParentFLAIRDeviceUploadID|CarelinkIndex|DataDtTm|CGM|SensorCal|ISIG|DataDtTm_adjusted|Unusuable|UnusableReason
1|26|144|18164|5/15/2019 9:18:15 PM|136||27.47||False
2|26|144|18165|5/15/2019 9:13:15 PM|146||29.02||False
3|26|144|18166|5/15/2019 9:08:15 PM|157||30.48||False
4|26|144|18167|5/15/2019 9:03:15 PM|166||31.75||False
5|26|144|18168|5/15/2019 8:58:15 PM|174||32.6||False
6|26|144|18169|5/15/2019 8:53:15 PM|183||33.21||False
7|26|144|18170|5/15/2019 8:48:15 PM|193||33.83||False
8|26|144|18171|5/15/2019 8:43:15 PM|202||34.55||False
9|26|144|18172|5/15/2019 8:38:15 PM|208||35.09||False
10|26|144|18173|5/15/2019 8:33:15 PM|207||35.02||False
11|26|144|18174|5/15/2019 8:28:15 PM|203||34.6||False
12|26|144|18175|5/15/2019 8:23:15 PM|197||33.61||False
13|26|144|18176|5/15/2019 8:18:15 PM|197||33.04||False
14|26|144|18177|5/15/2019 8:13:15 PM|201||33.18||False
15|26|144|18178|5/15/2019 8:08:15 PM|204||33.27||False
16|26|144|18179|5/15/2019 8:03:15 PM|197||32.61||False
17|26|144|18180|5/15/2019 7:58:15 PM|191||31.94||False
18|26|144|18181|5/15/2019 7:53:15 PM|189||31.39||False
19|26|144|18182|5/15/2019 7:48:15 PM|188||31.08||False
20|26|144|18183|5/15/2019 7:43:15 PM|189||31.15||False
21|26|144|18184|5/15/2019 7:38:15 PM|187||31.12||False
22|26|144|18185|5/15/2019 7:33:15 PM|182||30.76||False
23|26|144|18186|5/15/2019 7:28:15 PM|179||30.5||False
24|26|144|18187|5/15/2019 7:23:15 PM|180||30.67||False
25|26|144|18188|5/15/2019 7:18:15 PM|188||31.24||False
26|26|144|18189|5/15/2019 7:13:14 PM|197||31.87||False
27|26|144|18190|5/15/2019 7:08:14 PM|205||32.28||False
28|26|144|18191|5/15/2019 7:03:14 PM|211||32.99||False
29|26|144|18192|5/15/2019 6:58:14 PM|212||33.31||False
30|26|144|18193|5/15/2019 6:53:14 PM|209||33.11||False
31|26|144|18194|5/15/2019 6:48:14 PM|205||32.91||False
32|26|144|18195|5/15/2019 6:43:14 PM|203||32.83||False
33|26|144|18196|5/15/2019 6:38:14 PM|207||33.3||False
```

Figure 3.1: CGM data series format

### 3.3.2 Simulation Result

Recall our model 2.2.1

$$\frac{dG_1(t)}{dt} = -\alpha G_1(t)$$
$$\frac{dG_2(t)}{dt} = \alpha G_1(t) - \left(\beta_1 + \beta_2 \left(\bar{I}(t) + I_b\right)\right) G_2(t)$$
$$\frac{d\bar{I}(t)}{dt} = \gamma \ln\left(\exp\left(G_2(t) - T_{upper}\right) + 1\right) - \delta \bar{I}(t)$$

| Symbol | Meaning | Unit |
|---|---|---|
| $G_1(t)$ | Glucose disturbance of the digestive system at time $t$ | mg/dl |
| $G_2(t)$ | Glucose disturbance in the blood at time $t$ | mg/dl |
| $I(t)$ | The effective insulin level at time $t$ | $\mu$U/ml |
| $I_b$ | Basal insulin level | $\mu$U/ml |
| $\bar{I}(t)$ | Rapid-acting insulin level at time $t$ | $\mu$U/ml |

Continued on next page

**Table 3.1 continued from previous page**

| Symbol | Meaning | Unit |
|---|---|---|
| $T_{upper}$ | Threshold for high blood glucose concentration | mg/dl |
| $T_{lower}$ | Threshold for low blood glucose concentration | mg/dl |
| $G_2^{\text{obs}}(t)$ | Observed data of $G_2$ at time $t$ | mg/dl |
| $u(t)$ | Insulin pump dosage at time $t$ | $\mu$U/ml |
| $\alpha$ | Rate constant of decreasing glucose level in the digestive system | mg/dl/h |
| $\beta_1$ | Rate constant of hormone-independent decrease of glucose level in the blood | mg/dl/h |
| $\beta_2$ | Rate constant of hormone-dependent decrease of glucose level in the blood | mg/dl/h |
| $\gamma$ | Rate constant of release of hormone due to blood glucose disturbance | $\mu$U/ml/h |
| $\delta$ | Rate constant for removal of hormone due to disturbance of blood hormone level | $\mu$U/ml/h |

Table 3.1: List of Notation

The value of $T_{upper}$ is taken as 110 mg/dl. Our proposal involves conducting simulations for two groups of people: healthy individuals and those with diabetes. Our aim is to identify and compare the parameters of the mathematical models used for each group, in order to understand the differences in their metabolic dynamics.

First, we show the simulation results for a 6-hour period, from 6 a.m (the time of breakfast) to 12 p.m, in Figures 3.2 and 3.3. The initial blood glucose concentrations are 70 mg/dl for the normal person and 100 mg/dl for the diabetic person. The initial values of glucose in the digestive system are 120 mg/dl for the normal person and 100 mg/dl for the diabetic person. The initial quick effective insulin concentration for both individuals is set to 0

$\mu$U/dl and the insulin basals are 10 and 5 $mu$U/dl, respectively.

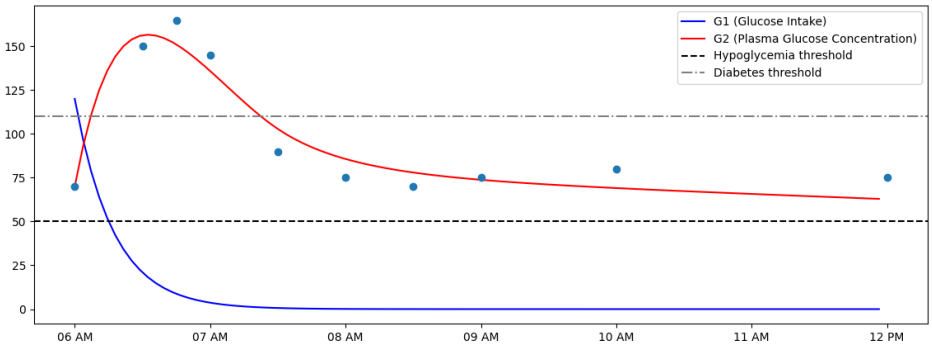


Figure 3.2: Simulation for a healthy person in 6 hours

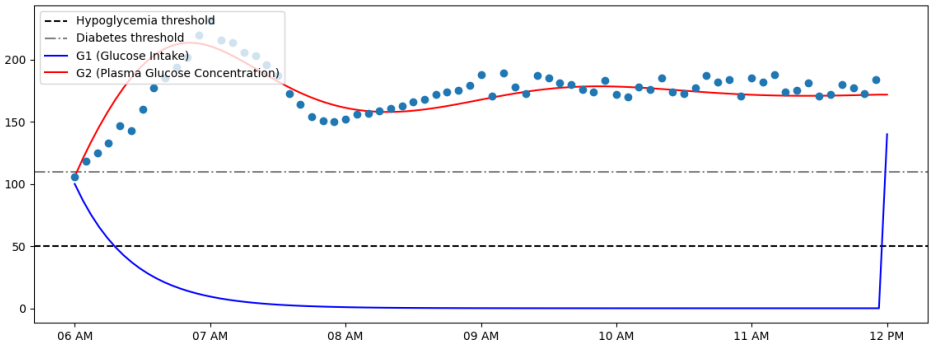


Figure 3.3: Simulation for a diabetic person in 6 hours

The parameter values are shown in 3.2. Comparing the parameter estimation values of a healthy person and a diabetic person, we can see that there are significant differences in the values of $\beta_2$ and $\gamma$. The value of $\beta_2$ is higher for the healthy person, indicating a higher rate of insulin sensitivity, while the value of $\gamma$ is much higher for the healthy person, indicating a more efficient regulation of glucose by insulin. On the other hand, the value of $\beta_1$ is slightly higher for the diabetic person, indicating a lower rate of insulin secretion. The

other parameters, $\alpha$ and $\delta$, also show some differences, but they are relatively small compared to the differences in $\beta_2$ and $\gamma$. Overall, these parameter values provide important insights into the physiological differences between a healthy person and a diabetic person, which can inform the development of personalized treatment strategies.

Table 3.2: Parameter Estimation Values

| | Healthy Person | Diabetic Person |
|---|---|---|
| $\alpha$ | 2.4897 | 2.3625 |
| $\beta_1$ | 0.4559 | 0.4769 |
| $\beta_2$ | 0.6635 | 0.2998 |
| $\gamma$ | 1.6307 | 0.0888 |
| $\delta$ | 0.2 | 1.3100 |

The simulation is extended to cover a whole day with three meals, which include breakfast at the starting point, lunch at 12 p.m., and dinner at 8 p.m. The glucose levels in the digestive system are assumed to be similar to those in the previous simulation for breakfast, while for lunch and dinner, 150 mg/dl glucose is assumed to be added to the digestive system immediately. The results of the simulation for a normal person and a diabetic person are presented in Fig 3.4 and 3.5, respectively. We assume that there is no metabolism of glucose in the body at night, starting from 11 p.m. Therefore, the concentration of glucose at the beginning of the next morning remains nearly the same.

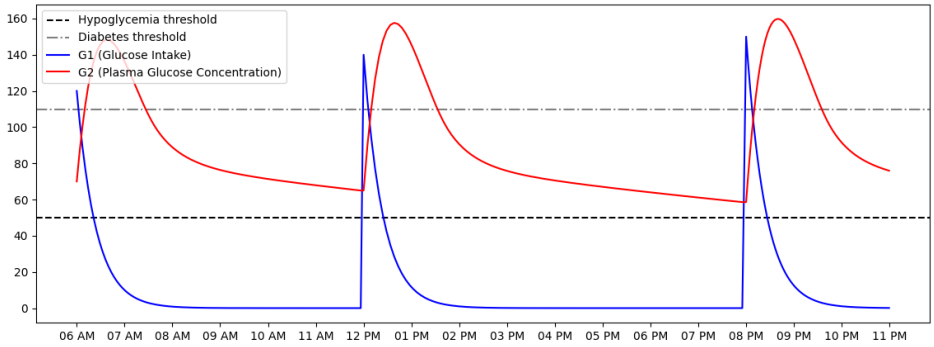


Figure 3.4: Simulation for a healthy person in a day

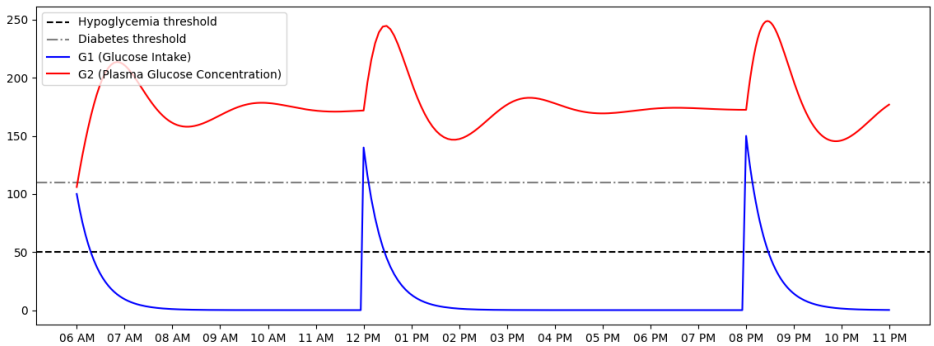


Figure 3.5: Simulation for a healthy person in a day

# Chapter 4

# Control Insulin Dose

In this section, we will focus on insulin dose therapy by a pump machine, which pumps insulin into the body continuously. We emphasize this to distinguish with the insulin dose three times a day, before the meal. This method is much more flexible than the traditional method of insulin injection three times as it allows for more precise and individualized dosing of insulin throughout the day. The pump can be programmed to deliver different doses of insulin at different times, depending on the individual's needs. Additionally, the pump can provide a continuous infusion of insulin, which more closely mimics the natural insulin production of a healthy pancreas. Overall, insulin pump therapy provides a safe and effective way to manage diabetes and improve the quality of life for those living with this condition.

## 4.1 Derivation

This section is dedicated to determining the appropriate insulin dosage for treating diabetes through insulin injection. Medical guidelines define the "normal" range for blood glucose concentration as between 70 to 110 (mg/dl),

with levels below this threshold labeled as hypoglycemia and levels above the upper limit considered hyperglycemia. In a normal body, after food consumption, the blood glucose level temporarily goes above this range but returns to normal within 2-3 hours. However, for diabetic patients, it takes 4-5 hours for glucose levels to return to normal. Insulin bolus therapy involves pumping extra quick-acting insulin into the body to expedite the process of reducing glucose levels to the normal range. From a mathematical modeling perspective, the control variable, denoted as $u(t)$, represents the insulin pump dosage as a function of time

$$\begin{aligned}
\frac{dG_1(t)}{dt} &= -\alpha G_1(t) \\
\frac{dG_2(t)}{dt} &= \alpha G_1(t) - \left(\beta_1 + \beta_2 \left(\bar{I}(t) + I_b\right)\right) G_2(t) \\
\frac{d\bar{I}(t)}{dt} &= \gamma \ln\left(\exp\left(G_2(t) - T_{upper}\right) + 1\right) - \delta \bar{I}(t) + u(t)
\end{aligned} \tag{4.1.1}$$

to minimize the objective function

$$\int_0^T (G_2(t) - T_{lower})(G_2(t) - T_{upper}) + \frac{1}{2}u^2(t)dt$$

This problem can be considered an optimal control problem in mathematics. A control policy of $0 \leq u(t) \leq 200$ ($\mu$U/ml) can be applied. The objective function is set such that $G_2(t)$ is within the range of $[T_{lower}, T_{upper}]$ for the maximum feasible time. This approach is intended to expedite the process of reducing glucose levels. The component $\frac{1}{2}u^2(t)$ is used as a regularization term.

## 4.2 Background on Optimal Control

Formally, for parameter $\theta \in \mathbb{R}^n$, consider optimal control problem $\Sigma(\theta)$, including

$$\begin{aligned}
&\text{dynamics:} \quad \frac{d\boldsymbol{x}(t)}{dt} = \boldsymbol{f}\left(\boldsymbol{x}(t), \boldsymbol{u}(t), \boldsymbol{\theta}\right) \text{ with given } \boldsymbol{x}_0, \\
&\text{control policy :} \quad \frac{d\boldsymbol{u}(t)}{dt} = \boldsymbol{u}\left(t, \boldsymbol{x}(t), \boldsymbol{\theta}\right) \\
&\text{control objective:} \quad J(\boldsymbol{\theta}) = \int_0^T g(\boldsymbol{x}(t), \boldsymbol{u}(t), \boldsymbol{\theta}) dt + h\left(\boldsymbol{x}(T), \boldsymbol{\theta}\right)
\end{aligned} \tag{4.2.1}$$

Here, $\boldsymbol{x}(t) \in \mathbb{R}^n$ is the system state; $\boldsymbol{u}(t) \in U \subseteq \mathbb{R}^m$ is the control input; $\boldsymbol{f} : \mathbb{R}^n \times \mathbb{R}^m \times \mathbb{R}^r \mapsto \mathbb{R}^n$ is the dynamics model, which is assumed to be twice-differentiable; $t = 0, 1, \cdots, T$ is the time step with $T$ being the time horizon; and $J(\boldsymbol{\theta})$ is the control objective function with $g : \mathbb{R}^n \times \mathbb{R}^m \times \mathbb{R}^r \mapsto \mathbb{R}$ and $h : \mathbb{R}^n \times \mathbb{R}^r \mapsto \mathbb{R}$ denoting the stage/running and final costs, respectively, both of which are twice-differentiable. For a choice of $\boldsymbol{\theta}, \boldsymbol{\Sigma}(\boldsymbol{\theta})$ will produce a trajectory of state-inputs:

$$\boldsymbol{\xi}_{\boldsymbol{\theta}} = \left\{\boldsymbol{x}_{0:T}^{\boldsymbol{\theta}}, \boldsymbol{u}_{0:T-1}^{\theta}\right\} \in \arg \min_{\{\boldsymbol{x}_{0:T}, \boldsymbol{u}_{0:T-1}\}} J(\boldsymbol{\theta}) \tag{4.2.2}$$

that is, $\boldsymbol{\xi}_{\boldsymbol{\theta}}$ optimizes $J(\boldsymbol{\theta})$ subject to the dynamics and control policy constraint. If $\boldsymbol{u}(t) = \boldsymbol{u}\left(t, \boldsymbol{x}_t, \boldsymbol{\theta}\right)$ (i.e., feedback policy explicitly depends on $\boldsymbol{x}_t$), 4.2.2 is a close-loop optimal control problem; otherwise if $\boldsymbol{u}(t) = \boldsymbol{u}(t, \boldsymbol{\theta})$ (e.g., polynomial parameterization), 4.2.2 is an open-loop motion planning problem. To solve an optimal control problem, there are various approaches, as shown in Fig 4.1. In this thesis, we choose the approach of Indirect Methods utilizing Pontryagin Maximum Principle (PMP)

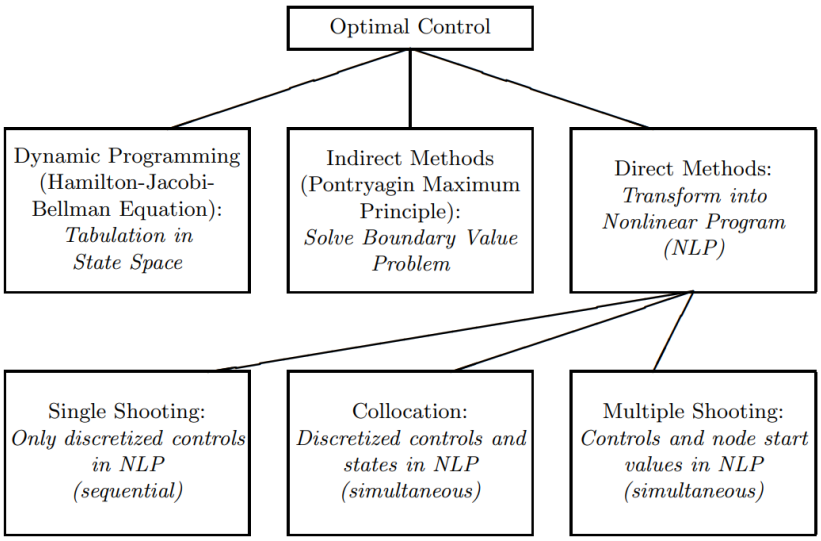


Figure 4.1: Optimal Control solver approach system

## 4.3 Utilizing PMP to solve insulin dose problem

To see the existence of optimal control, the following theorem is used

**Theorem 4.3.1.** *Consider the optimal control problem 4.2.1 on a fixed interval* $[0, T]$*. Assume that*

- *There exists an* $M > 0$*, such that* $\|x(t,u)\| \leq M$ *for all* $u \in \mathbf{U}$ *and* $0 \leq t \leq T$;
- $f$ *is lower semicontinuous;*
- $\mathbf{D}^+ = \{(y^0, y) : \exists v \in \mathbf{U}, y = f(t,x,v), y^0 \geq g(t,x,v)\}$ *is convex for* $(t,x) \in [0,T] \times \{|x| \leq M\}$

*Then there exists an optimal control* $u^* \in \mathbf{U}$*.*

Using this theorem, we could show the existence of optimal control for problem 4.1.1, since $L^\infty$ bounds hold for this system and the integrand of the objective function is convex.

The necessary condition for optimal control is obtained using Potryagin's Maximum Principle. To introduce these conditions, we first define the following Hamiltonian,

$$H(t, \boldsymbol{X}, \boldsymbol{u}) = g(t, \boldsymbol{X}, \boldsymbol{u}) + \boldsymbol{f}(t, \boldsymbol{X}, \boldsymbol{u})' \boldsymbol{\lambda},$$

where $\lambda \in \mathbb{R}^n$ is called the costate variable, which can be also thought of as the Lagrange multipliers for the dynamics constraints. The PMP states that there exists a costate $\lambda =: \lambda^\theta$, which together with the optimal trajectory $\boldsymbol{\xi}_\theta$ satisfies

$$\begin{cases} \lambda'(t) = -\frac{\partial H}{\partial x} \\ \lambda(T) = h'(x(T)), \qquad \text{transversality condition} \end{cases} \tag{4.3.1}$$

Applying the Hamiltonian for the control model 4.1.1, we have:

$$\begin{aligned} H = \quad & (G_2(t) - T_{lower})(G_2(t) - T_{upper}) + \frac{1}{2}u^2(t) + \lambda_1 \left(-\alpha G_1(t)\right) \\ & + \lambda_2 \left(\alpha G_1(t) - \left(\beta_1 + \beta_2 \left(\bar{I}(t) + I_b\right)\right) G_2(t)\right) \\ & + \lambda_3 \left(\gamma \ln\left(\exp\left(G_2(t) - T_{upper}\right) + 1\right) - \delta \bar{I}(t) + u(t)\right) \end{aligned}$$

where $\lambda_i \quad (i = 1, 2, 3)$ satisfies

$$\begin{cases} \lambda_1' = \alpha\lambda_1 - \alpha\lambda_2 \\ \lambda_2' = -2G_2(t) + (T_{\text{lower}} + T_{\text{upper}}) + \lambda_2\beta_2 \left(\bar{I}(t) + I_b\right) - \lambda_3\gamma V \\ \lambda_3' = \lambda_2\beta_2 G_2(t) \\ \lambda_1(T) = \lambda_2(T) = \lambda_3(T) = 0 \end{cases} \tag{4.3.2}$$

Here we use the notation

$$V = \frac{(G_2(t) - T_{\text{upper}})\, e^{G_2(t)-T_{\text{upper}}}}{e^{G_2(t)-T_{\text{upper}}} + 1}$$

Moreover we have

$$\frac{\partial H}{\partial u} = \lambda_3 + u = 0 \text{ at } u^* \text{ is optimal control solution}$$

Using upper and lower bound for control $u^*$, it can be seen that optimal control $u^*$ could be characterized as

$$u^* = \min\left\{u_{upper}, (-\lambda_3)^+\right\},$$

where $\kappa^+ = \kappa$ if $\kappa \geq 0, \kappa^+ = 0$ if $\kappa < 0$. So we reach the optimality system

$$\begin{cases} \frac{dG_1(t)}{dt} = -\alpha G_1(t) \\ \frac{dG_2(t)}{dt} = \alpha G_1(t) - \left(\beta_1 + \beta_2\left(\bar{I}(t) + I_b\right)\right) G_2(t) \\ \frac{d\bar{I}(t)}{dt} = \gamma \ln\left(\exp\left(G_2(t) - T_{upper}\right) + 1\right) - \delta \bar{I}(t) + \min\left\{u_{upper}, (-\lambda_3)^+\right\} \\ \lambda_1' = \alpha\lambda_1 - \alpha\lambda_2 \\ \lambda_2' = -2G_2(t) + (T_{\text{lower}} + T_{\text{upper}}) + \lambda_2\beta_2\left(\bar{I}(t) + I_b\right) - \lambda_3\gamma V \\ \lambda_3' = \lambda_2\beta_2 G_2(t) \\ G_1(0) = G_{10}, G_2(0) = G_{20}, \bar{I}(0) = \bar{I}_0 \\ \lambda_1(T) = \lambda_2(T) = \lambda_3(T) = 0 \end{cases} \tag{4.3.3}$$

which could be solved by numerical method (e.g: Runge-Kutta method). We use the following parameters and conditions

| Parameter | Value |
|---|---|
| $\alpha$ | 2.3624595 |
| $\beta_1$ | 0.47694835 |
| $\beta_2$ | 0.29979771 |
| $\gamma$ | 0.08884565 |
| $\delta$ | 1.31002741 |
| $T_{upper}$ | 110 |
| $T_{lower}$ | 50 |
| $u_{upper}$ | 250 |
| $I_b$ | 5 |

| Initial Condition | Value |
|---|---|
| $G_{10}$ | 100 |
| $G_{20}$ | 100 |
| $\bar{I}_0$ | 0 |

Table 4.1: Parameters and Initial Conditions

For practice, in 2020, Pontryagin-Differentiable-Programming framework was introduced by Jin et al. [7] as a means of solving optimal control problems. This framework was developed in response to the need for an end-to-end learning approach that unifies learning and control by integrating deep neural networks with the Pontryagin's Maximum Principle (PMP). Utilizing this framework at https://github.com/wanxinjin/Pontryagin-Differentiable-Programming [14] for insulin bolus therapy for the diabetic person in Chapter 5, we have the control result 4.2

The findings from our study indicate that during the initial phase of a meal, it is crucial to administer approximately 70 $\mu$U/dl units of insulin to the body. This particular time period corresponds to the peak of blood glucose levels, where the naturally produced quick-acting insulin by the pancreas may not be sufficient to regulate the glucose effectively. Within just one hour, the blood glucose levels return to the normal range. As the digestion process progresses and all the glucose from the digestive system enters the bloodstream, the insulin dosage can be reduced to around 10 $\mu$U/dl. This adjustment aligns with the physiological changes that occur after ap-

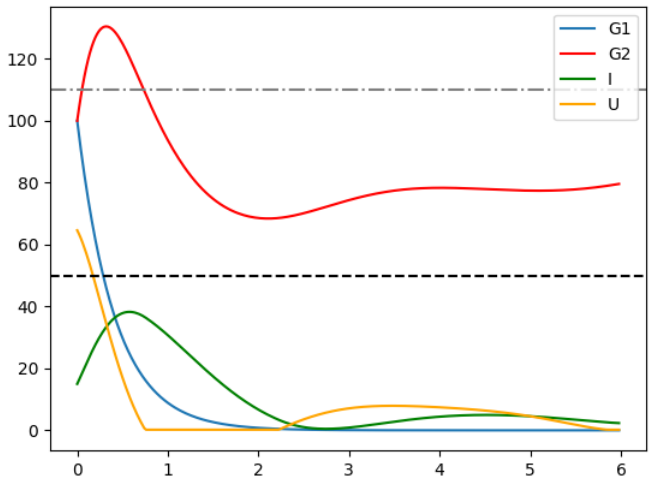


Figure 4.2: Insulin Bolus Strategy in 6 hours for a diabetic person

proximately two hours following a meal. By closely examining the proposed insulin therapy approach, we observe a remarkable correspondence between our findings and real-life observations. This demonstrates the effectiveness of our proposed therapy in accurately capturing the dynamics of glucose metabolism and insulin requirements in practical scenarios.

# Conclusion

In this thesis, we have made several contributions. First, we provided an overview of the basic knowledge of diabetes, including the dynamic metabolism of glucose and hormone insulin in the body. Second, we developed a new mathematical model that accurately captures the dynamics of glucose and insulin in the human body. Third, we personalized the model parameters for each patient by combining Subject Matter Expertise (SME) and Gauss-Newton Algorithm based on their individual characteristics and medical history. Finally, we proposed an insulin bolus strategy that optimizes blood glucose control for each patient based on the personalized model in the context of optimal control problem using the Pontryagin Maximal Principle. This study represents a novel direction in diabetes research, and has important implications for medical practice. Firstly, the proposed mathematical model provides a simulation laboratory that doctors can use to test and refine their treatment plans for patients. By simulating the model, treatments can be tested and optimized without exposing real patients to potential harm. Secondly, the model enables a more precise and individualized dosing of insulin, as opposed to the previous approximation-based dosing methods. This advance has significant potential to improve the safety and efficacy of insulin therapy for diabetic patients.

In future studies, several directions could be explored. Firstly, it would be interesting to administer the therapy of injections three times a day with meals, with one injection given every other day, for other types of diabetes therapy. Secondly, it would be worth investigating the use of a mixed dose

of fast-acting and intermediate-acting insulin. Additionally, the mathematical model could be expanded further by considering a larger model. One potential approach involves constructing a model that incorporates a system of differential equations, accounting for factors such as the impact of a mixed meal and the glycogen stored compartment. This can be represented as follows

$$
\begin{aligned}
&E(t) = A_g(t) + A_F\left(\text{Relu}\left(t-\tau_1\right)\right) + A_l\left(\text{Relu}\left(t-\tau_2\right)\right)\\
&\begin{cases}
\frac{dG_D}{dt} = -\frac{G_D(t)}{\alpha_1} + E(t)\\
\frac{dG_B}{dt} = \frac{G_D(t)}{\alpha_1} - \alpha_2 G_B(t) - \alpha_3 I(t) G_B(t) + Y(t)
\end{cases}\\
&\frac{dY}{dt} = \alpha_4\left(\alpha_2 G_B(t) - \alpha_5 Y(t)\right) - \beta R(t) Y(t)\\
&\begin{cases}
\frac{dI}{dt} = \frac{1}{\beta_1}\left(-I(t) + \varphi\left(V_i(t) + V_{s_c}\left(\text{ReLu}\left(t-r_3\right)\right)\right)\right)\\
\frac{dS}{dt} = \frac{1}{\beta_2}\left(\left(-S(t)\right) + V_{sc}(t)\right)\\
\frac{dR}{dt} = \frac{1}{\beta_3}\left(-R(t) + Y(t)\right)
\end{cases}
\end{aligned}
$$

This expanded model can provide a more comprehensive understanding of glucose and insulin dynamics in the human body.

# Bibliography


[1] Chowdhury, Sourav, et al. "Mathematical Model of ingested glucose in Glucose-Insulin Regulation." arXiv preprint arXiv:2003.02573 (2020).

[2] Goel, Pranay, et al. "A minimal model approach for analyzing continuous glucose monitoring in type 2 diabetes." Frontiers in physiology 9 (2018): 673.

[3] Fabietti, Pier Giorgio, et al. "Control oriented model of insulin and glucose dynamics in type 1 diabetics." Medical and Biological Engineering and Computing 44.1 (2006): 69-78.

[4] Jonathan Calver. "Parameter estimation for ordinary differential equations." CAIMS (2019).

[5] Bergman RN, Ider YZ, Bowden CR, Cobelli C: Quantitative Estimation of Insulin Sensitivity. Am J Physiol 1979, 23(6):E667-E677.

[6] Derouich M, Boutayeb A: The effect of physical exercise on the dynamics of glucose and insulin. Journal of Biomechanics 2002, 35:911-917.

[7] Jin, Wanxin, et al. "Pontryagin differentiable programming: An end-to-end learning and control framework." Advances in Neural Information Processing Systems 33 (2020): 7979-7992.

[8] Palumbo, P., Ditlevsen, S., Bertuzzi, A., De Gaetano, A. (2013). Mathematical modeling of the glucose–insulin system: A review. Mathematical biosciences, 244(2), 69-81.

[9] S. Gugushvili, C.A.J. Klaassen, et al. $\sqrt{n}$-consistent parameter estimation for systems of ordinary differential equations: bypassing numerical integration via smoothing. Bernoulli, 18(3): 1061–1098, 2012.

[10] Cartwright, J. H., Piro, O. (1992). The dynamics of Runge–Kutta methods. International Journal of Bifurcation and Chaos, 2(03), 427-449.

[11] Diehl, Moritz, et al. "Fast direct multiple shooting algorithms for optimal robot control." Fast motions in biomechanics and robotics: optimization and feedback control (2006): 65-93.

[12] Joshi, Hem Raj, et al. "Optimal control methods applied to disease models." Contemporary Mathematics 410 (2006): 187-208.

[13] Mary Martin, Elizabeth Chun, David Buchanan, Rucha Bhat, Shaun Cass, Eric Wang, Sangaman Senthil Irina Gaynanova. (2021, April 27). irinagain/Awesome-CGM: List of public CGM datasets (Version v1.1.0). Zenodo.

[14] Jin, Wanxin et al. "Pontryagin differentiable programming: An end-to-end learning and control framework". Advances in Neural Information Processing Systems 33. (2020): 7979–7992.

[15] Bertuzzi, A., Salinari, S., Mingrone, G.: Insilin granule traffickin in -cells: mathematical model of glucose-induced insulin secretion. Am. J. Physiol. Endocrinol.Metab., 293: E396-E409 (2007)